Annals of R.S.C.B., ISSN:1583-6258, Vol. 25, Issue 4, 2021, Pages. 3460 - 3473
Received 05 March 2021; Accepted 01 April 2021.

A Framework of Common Coupling through an Ac– Dc–Ac Back-To-Back Converter Set

Pokala Pranay Kumar
Research Scholar, Dept. of Electrical & Electronics Engineering,
Sri Satya Sai University of Technology & Medical Sciences,
Sehore, Bhopal-Indore Road, MadhyaPradesh, India

Dr. A S Rathore
Research Guide, Dept. of Electrical & Electronics Engineering,
Sri Satya Sai University of Technology & Medical Sciences,
Sehore, Bhopal-Indore Road, MadhyaPradesh, India

Abstract

HIGH power converters utilized in modern and power framework applications utilize appropriation of power among numerous power semiconductor gadgets. Progressions in the unique topologies of power converters give extra advantages of high dependability, excess and better out power quality. Worry of power quality in power frameworks has acquired extensive consideration in past decade. Accordingly these uncommon topologies of power-electronic converters are progressively utilized in power moulding, power sifting, electrical drives, appropriated age applications and advancement of electric drive trains for enormous vehicles. There are numerous converter topologies that go under the two phases of the AC/DC/AC converter.Lattice interface or utility provided power conversion chiefly includes either AC to DC, DC to AC or mix of both the converters. An AC to DC to AC converter or AC/DC/AC framework interfaces two AC subsystems utilizing two phase power conversions that is from AC to DC and afterward DC to AC.

Introduction

Power electronics makes up an enormous piece of designing and has close associations with numerous territories of physical science, science, and mechanics. It builds up a quickly growing field in electrical designing and an extent of its innovation covers a wide range. Power applications with electronic converters do a ton of troublesome work for us. Hopeful people imagine power electronics accomplishing an ever increasing number of things for the populace. Electronic machines add to a better and more agreeable live the world over.Thanks to propels in science and related innovation, numerous individuals at this point don't need to invest a lot of

Annals of R.S.C.B., ISSN:1583-6258, Vol. 25, Issue 4, 2021, Pages. 3460 - 3473
Received 05 March 2021; Accepted 01 April 2021.

energy working for the minimum essentials of life. Whatever it is that we truly need to do, power electronics causes us to improve.

Back-to-Back Converter

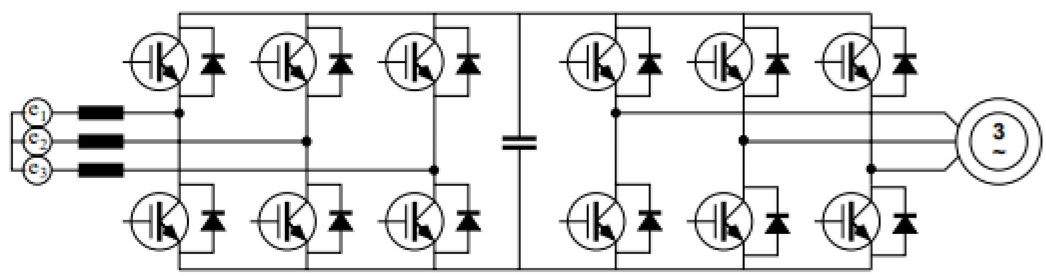

Figure 1. Back-to-Back Converter

It consists simply of a force-commutated rectifier and a force-commutated inverter connected with a common dc-link, see figure 1.1. The properties of this combination are well known; the line-side converter may be operated to give sinusoidal line currents, for sinusoidal currents, the dc-link voltage must be higher than the peak main voltage, the dc-link voltage is regulated by controlling the power flow to the ac grid and, finally, the inverter operates on the boosted dc-link, making it possible to increase the output power of a connected machine over its rated power. Another advantage in certain applications is that braking energy can be fed back to the power grid instead of just wasting it in a braking resistor.

An important property of the back-to-back converter is the possibility of fast control of the power flow. By controlling the power flow to the grid, the dc-link voltage can be held constant. The presence of a fast control loop for the dc-link voltage makes it possible to reduce the size of the dc-link capacitor, without affecting inverter performance. In fact, the capacitor can be made small enough to be implemented with plastic film capacitors.

Literature Review

Adamali Shah and Al-Numay have proposed a discrete - time model for spasmodic conduction mode of the PWM DC-DC converter. The cycle to cycle conduct of the framework is read for shifting the exchanging frequencies and burden protections. This model precisely reenacts the normal conduct of the yield voltage.

Annals of R.S.C.B., ISSN:1583-6258, Vol. 25, Issue 4, 2021, Pages. 3460 - 3473
Received 05 March 2021; Accepted 01 April 2021.

Xiongfei Wang et al have modelled and broke down the harmonic soundness of three phase inverter in a power framework. This methodology is valuable for the investigation of harmonic unsteadiness in a power electronic based power framework. The consequences of non straight time space re-enactments and hypothetical examination in the frequency area dependent on the linear zed models of inverters with internal control circles approve the viability of this plan.

HoucineMiloudi et al have proposed an insightful technique to model acceptance machines and the links interfacing the converter to the machine for electromagnetic similarity examination. They assembled a high frequency model utilizing FDA and it is utilized to register the high frequency spillage flow which causes the EMI in electronic and electric gear.

KapatSantanu has proposed a reconfigurable bi-frequency DPWM regulator to spread the power range with unsurprising wave boundaries. The discrete time modeling of the converter examinations the dependability of the proposed converter and equipment is executed utilizing FPGA for coordinated buck converter.

Methodology

The essential ideas of existing PWM strategies and created strategies are imagined hypothetically with the help of mathematical relations. The functionality of the strategies is confirmed through MATLAB 7.10 (2010a)/Simulink tool based simulation. The proposed strategies are actualized in a Field Programmable Gate Array (FPGA) processor. ModelSim 6.3 is utilized as a tool for performing functional simulation while Xilinx ISE 13.2 is the combine tool for the Register Transfer Level (RTL) confirmation and usage. The functional confirmed code of the architecture is downloaded to the Spartan-6 FPGA (XC6SLX45) gadget.

The current day frameworks are powered by non-ideal sources whose yield impedance isn't immaterial, other than the vast majority of the loads are non-direct in nature (UffeBorup et al 2001). Additionally the inclusion of exchanged mode power converters makes the frameworks variable organized. The investigation of harmonic segments is an unavoidable piece of the examination, because of the prerequisites of higher power quality. Numerical strategies offer a decent portrayal of the non-trademark waveform twisting produced by the converters. The most generally utilized technique to compute the harmonic parts is a numerical time domain

Annals of R.S.C.B., ISSN:1583-6258, Vol. 25, Issue 4, 2021, Pages. 3460 - 3473
Received 05 March 2021; Accepted 01 April 2021.

simulation strategy, in which the different segments are investigated by addressing differential conditions.

The time domain strategies are not difficult to utilize and permit confirmation of framework operation under quite a few diverse working states. Anyway they don't give a scientific understanding needed to optimal plan; other than frequency reliance can't be precisely modelled (Wood &Arrillaga 1995a, 1995b). An elective technique for computing the harmonic flows of a power converter utilizes the Fourier arrangement and the exchanging capacities. With a frequency domain model, the shut circle frequency responses can be set up, which will encourage the examination of framework solidness and plan optimization. The frequency response test is bulky to perform, for frameworks with enormous time constants, as the time needed for the yield to arrive at the consistent state for every frequency of the test signal is extremely long. Anyway frequency domain modelling is critical for power electronic circuits, which offer a quicker response.

An average Single Phase Diode Rectifier (SPDR) is appeared in Figure 2. By and large the rectifier works as a power converter, since its primary capacity is to change over the principal power frequency AC (50 or 60 Hz) to DC. The modulation is accomplished by the other exchanging activity of the diodes. The prompt yield voltage, V_{dc} shown in Figure 3 (c), is expressed in terms of the rectifier switching function 'S' and AC source voltage, V_{ac} as in Equation (1). Figure 3 (b) shows the exchanging capacity of the SPDR, which addresses the exchanging of the other diode sets, to interface the stock voltage to the DC-transport. This exchanging capacity works as a frequency transfer work in that it portrays the manner in which an AC side frequency signal is transferred to the DC side. The Fourier arrangement of exchanging capacity is given in Equation (2).

$$V_{dc} = V_{ac} * S$$

$$S = a_0 + \sum_{n=1} a_n \cos(n\omega t) + \sum_{n=1} b_n \sin(n\omega t)$$

As the switching function is symmetrical, the Fourier coefficients a_o and a_n area zero and the switching function S is

Annals of R.S.C.B., ISSN:1583-6258, Vol. 25, Issue 4, 2021, Pages. 3460 - 3473
Received 05 March 2021; Accepted 01 April 2021.

$$S = \sum_{n=1,3,..} \frac{4}{n\pi} \sin(n\omega t)$$

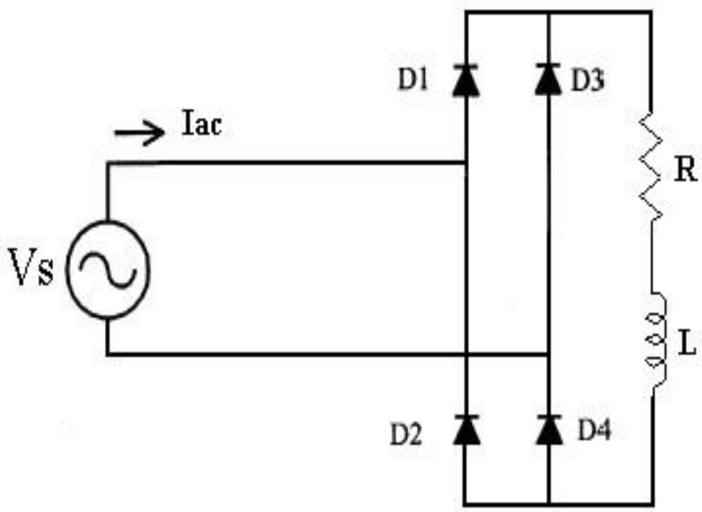

Figure 2 Unrestrained Rectifiers

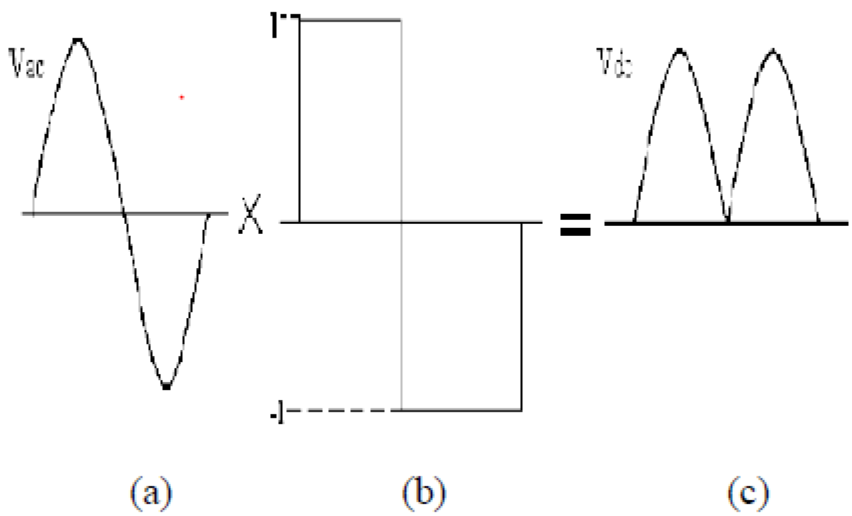

Figure 3 (a): Front end diode rectifier (b): Switching function and (c): Rectifier output

$$V_{dc} = \sum_{n=1,3,..} \frac{4}{n\pi} \sin(n\omega t) * V_m \sin(\omega t)$$

Annals of R.S.C.B., ISSN:1583-6258, Vol. 25, Issue 4, 2021, Pages. 3460 - 3473
Received 05 March 2021; Accepted 01 April 2021.

$$= \frac{2V_m}{\pi} - \frac{4V_m}{\pi} \sum_{n=2,4,\ldots} \frac{\cos(n\omega t)}{n^2 - 1}$$

The final rectifier output is given by above Equation and the rectifier load current is given by

$$I_{dc} = \frac{2V_m}{\pi R} - \frac{4V_m}{\pi} \sum_{n=1,2,3\ldots} \frac{\cos(2n\omega t)}{(4n^2-1)*Z_{2n}} \quad (4.6)$$

Where, Z_{2n} is the impedance offered to even order harmonic components. The rectifier source side current can also be obtained by using the same switching function (S) and the load side current, expressed as

$$I_{ac} = I_{dc} * S$$

$$I_{ac} = \frac{8V_m}{\pi^2 R} \sum_{n=1,3,5\ldots} \frac{\sin(n\omega t)}{n} - \frac{16V_m}{\pi^2} \sum_{n=1,2,3\ldots} \frac{\cos(2n\omega t)}{(4n^2-1)*Z_{2n}} * \sum_{n=1,3,5\ldots} \frac{\sin(n\omega t)}{n}$$

$$P_i^{th} \text{ intersection, } \alpha_m + \frac{\pi}{2M_f} M_a \sin\alpha_m - \frac{2j}{2M_f} = 0$$

$$P_{i+1}^{th} \text{ intersection, } \alpha_m - \frac{\pi}{2M_f} M_a \sin\alpha_m - \frac{2j}{2M_f} = 0$$

The Fourier coefficients for a pair of pulse is given as

$$B_n = \frac{4}{n\pi} \sin\left(\frac{n\delta_m}{4}\right) \left[\sin n\left(\alpha_m + \frac{3\delta_m}{4}\right) - \sin n\left(\pi + \alpha_m + \frac{\delta_m}{4}\right) \right]$$

Annals of R.S.C.B., ISSN:1583-6258, Vol. 25, Issue 4, 2021, Pages. 3460 - 3473
Received 05 March 2021; Accepted 01 April 2021.

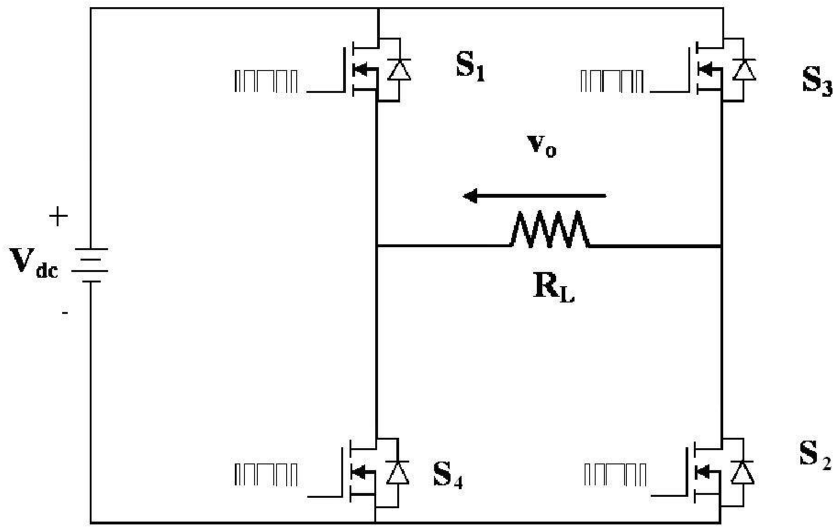

Figure 4 Single-phase full-bridge inverter

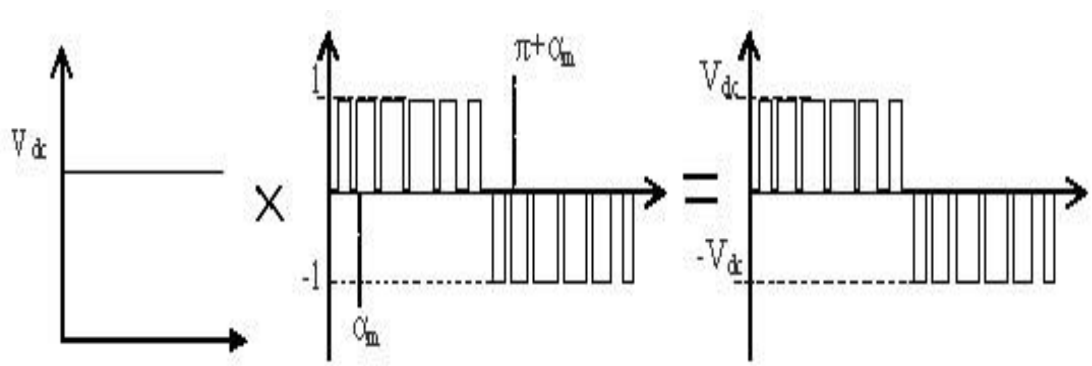

(a) **(b)** **(c)**

Figure 5 (a): Inverter input, (b): Switching function and (c): Inverter output

Where, α_m is the starting point of the pulse and δ_m the width of each pulse.The overall switching function is given as

$$S_I = \sum_{n=1.3.5..} \sum_{m=1}^{p} \frac{4}{n\pi} \sin\left(\frac{n\delta_m}{4}\right) \begin{bmatrix} \sin n\left(\alpha_m + \frac{3\delta_m}{4}\right) \\ -\sin n\left(\pi + \alpha_m + \frac{\delta_m}{4}\right) \end{bmatrix} \sin(n\omega t)$$

Annals of R.S.C.B., ISSN:1583-6258, Vol. 25, Issue 4, 2021, Pages. 3460 - 3473
Received 05 March 2021; Accepted 01 April 2021.

The output of the inverter is given by

$$V_o(t) = V_{dc} * S_I$$

$$V_o(t) = \sum_{n=1.3.5..}\sum_{m=1}^{p}\left(\frac{4V_{dc}}{n\pi}\sin\left(\frac{n\delta_m}{4}\right)\begin{bmatrix}\sin n\left(\alpha_m + \frac{3\delta_m}{4}\right) \\ -\sin n\left(\pi + \alpha_m + \frac{\delta_m}{4}\right)\end{bmatrix}\right)\sin(n\omega t$$

The inverter output current is the ratio between the output voltageand the load resistance, expressed as

$$I_o(t) = \sum_{n=1.3.5..}\sum_{m=1}^{p}\left(\frac{4V_{dc}}{n\pi R}\sin\left(\frac{n\delta_m}{4}\right)\begin{bmatrix}\sin n\left(\alpha_m + \frac{3\delta_m}{4}\right) \\ -\sin n\left(\pi + \alpha_m + \frac{\delta_m}{4}\right)\end{bmatrix}\right)\sin(n\omega t)$$

The inverter input current is obtained by using the inverter outputcurrent and the same switching function (S_I), given by

$$I_i(t) = I_o(t) * S_I$$

$$= \frac{V_{dc}}{R}\left[\sum_{n=1.3.5..}\sum_{m=1}^{p}\left(\frac{4}{n\pi}\sin\left(\frac{n\delta_m}{4}\right)\begin{bmatrix}\sin n\left(\alpha_m + \frac{3\delta_m}{4}\right) \\ -\sin n\left(\pi + \alpha_m + \frac{\delta_m}{4}\right)\end{bmatrix}\right)\sin(n\omega t)\right]^2$$

Annals of R.S.C.B., ISSN:1583-6258, Vol. 25, Issue 4, 2021, Pages. 3460 - 3473
Received 05 March 2021; Accepted 01 April 2021.

SIMULATION RESULTS

The simulation is performed on a SPWM inverter using MATLABboth in time and frequency domains for various values of M_a and M_f. The results obtained by the analytical method are compared with those available in the time domain for M_a=0.8 and M_f=10. The results are obtained for a rectifier of load resistance of 10Ω and inductance of 0.1H. The FDA results are moved in the Y-hub scale for clearness. Figure 6 (a) shows the DC voltage of the rectifier. It shows that the yield voltages utilizing FDA and TDA are practically the equivalent, however the yield DC current appeared in Figure 6 (b) uncovers that the TDA sets aside a more drawn out effort to arrive at the consistent state esteem.

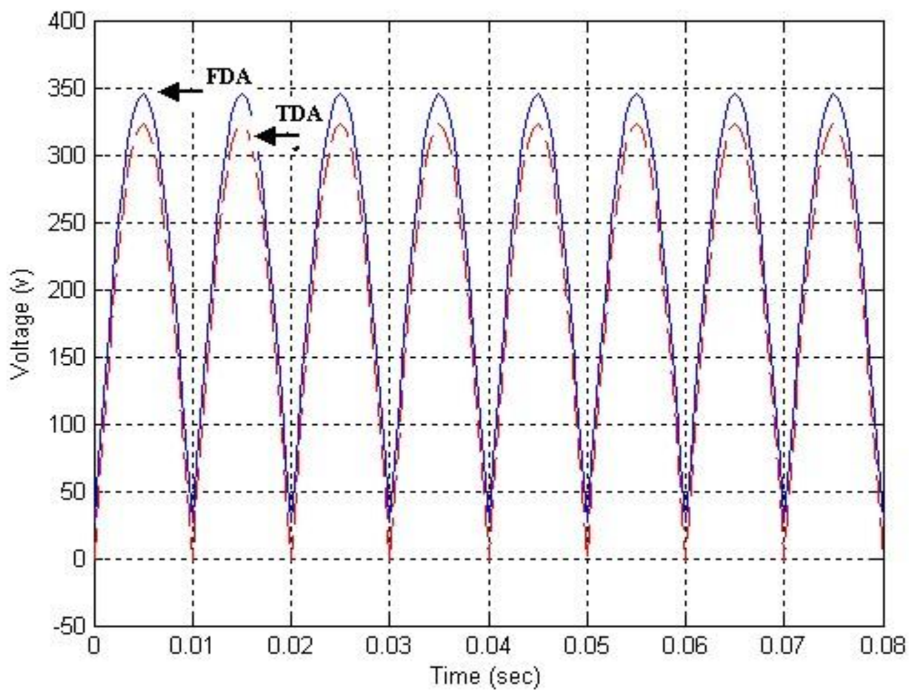

(a)

Annals of R.S.C.B., ISSN:1583-6258, Vol. 25, Issue 4, 2021, Pages. 3460 - 3473
Received 05 March 2021; Accepted 01 April 2021.

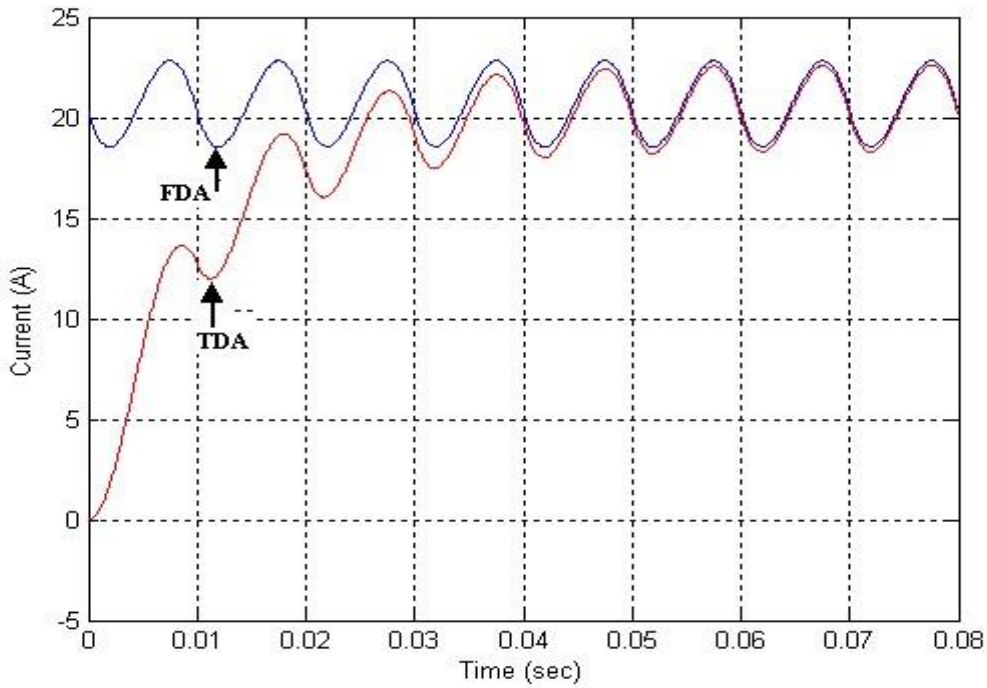

(b)

Figure 6 (a): Output voltage and (b): Output current waveform (FDA-calculated, TDA-replicated)

The source side current of the rectifier is found in Figure 6. The yield voltage of inverter and major segment of the yield are portrayed in Figure 7 (a) and (b) individually. Figure 8 shows the reproduced harmonic range of the inverter yield voltage. The prevailing harmonic parts of PWM controlled inverter are pushed to higher frequency true to form. It is seen that the inverter yield current waveform is equivalent to that of the voltage for a resistive burden.

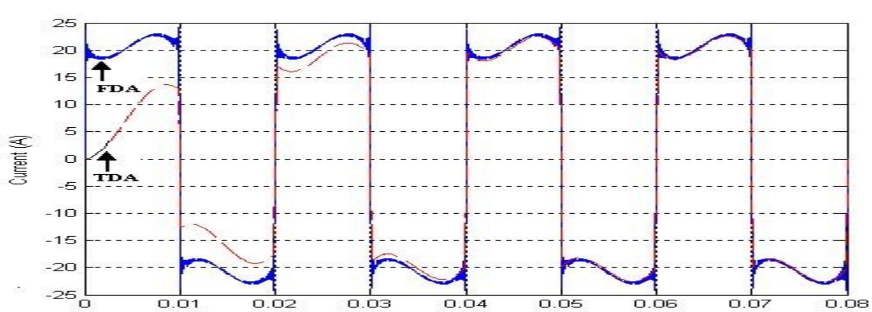

Figure 7 Foundation current waveform of rectifier (FDA -Calculated, TDA-simulated)

Annals of R.S.C.B., ISSN:1583-6258, Vol. 25, Issue 4, 2021, Pages. 3460 - 3473
Received 05 March 2021; Accepted 01 April 2021.

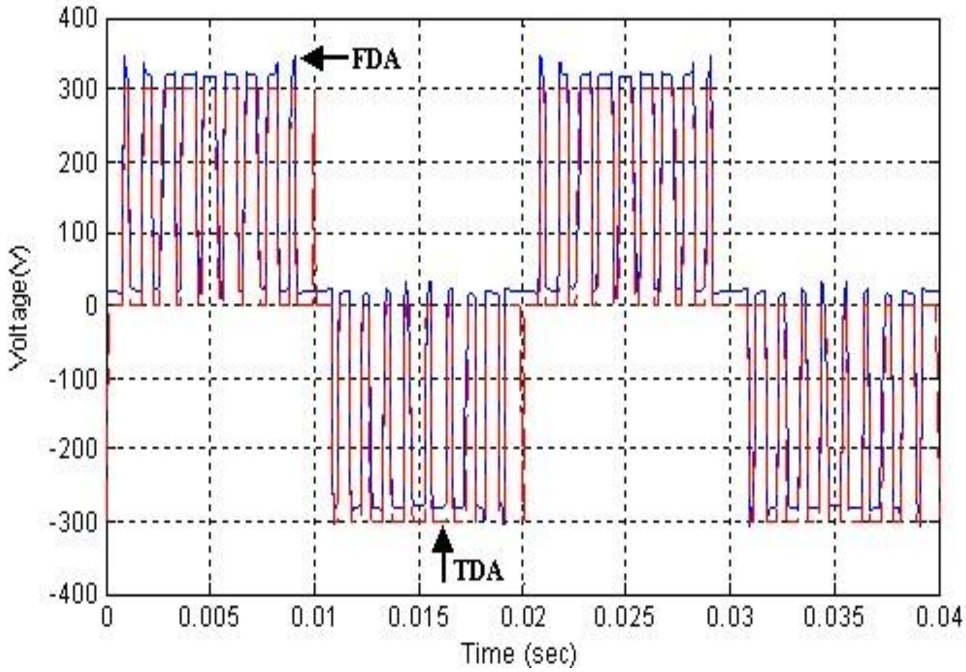

(a)

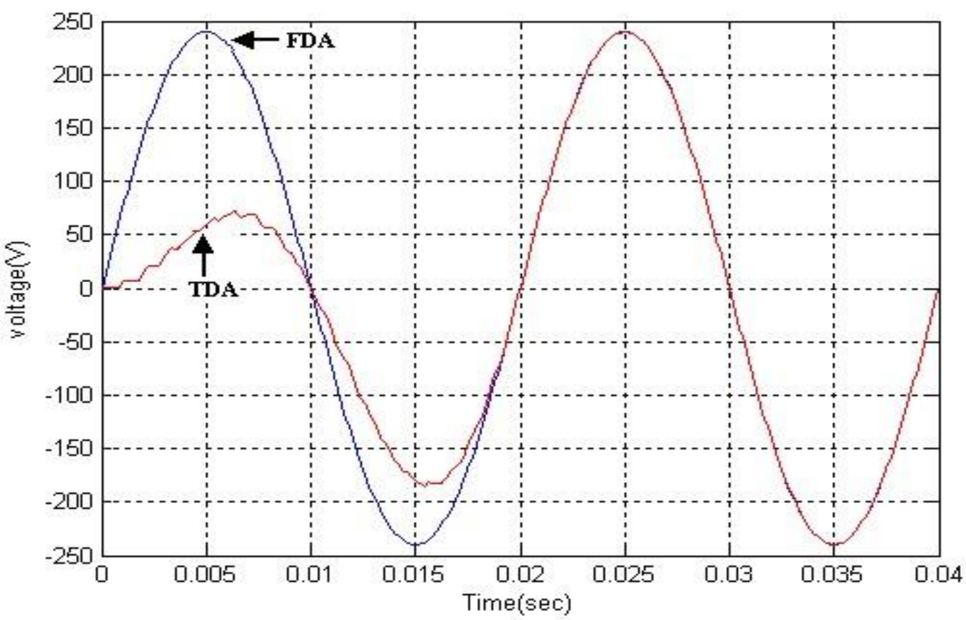

(b)

Figure 8 (a): Output voltage and (b): Fundamental component of output voltage (M_a= 0.8, M_f = 10, V_{dc} = 300V)

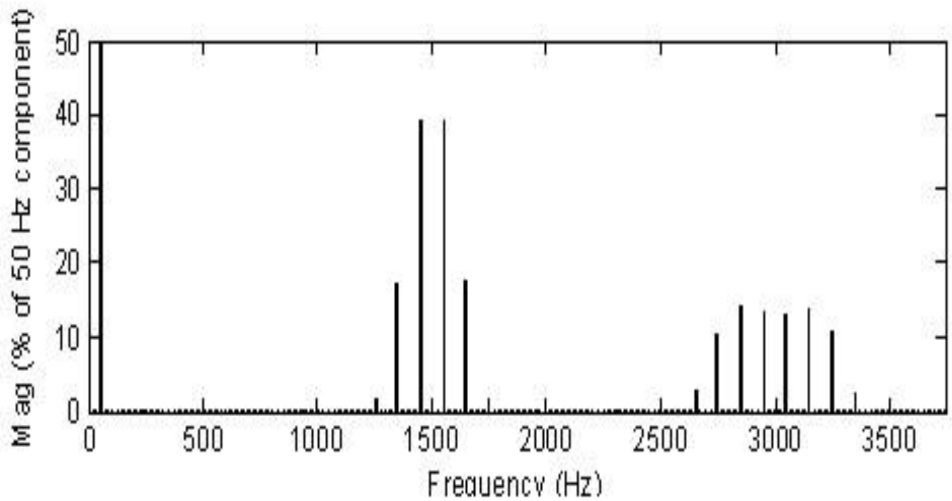

Figure 9 Harmonic spectrum of output voltage – SPWM M_a = 0.8, M_f = 15 and V_{dc} = 300V

Conclusion

The AC-DC-AC drive geography is having incredible favourable circumstances when contrasted with different classifications of AC-AC drives. It has gotten inescapable in engine drive applications. The critical favourable circumstances of the DC interface converters are uncontrolled rectifier at front end, accessibility of PWM strategies in wide execution range, direct flexibility of induction engine pivot change principle in VSI control and so forth In spite of the fact that AC-DC-AC drives have been grounded, still difficulties and openings exist in harmonic profile improvement, direct on-line elimination of current harmonics and so forth.The outcomes dependent on MATLAB simulation show that the yield current of rectifier in FDA arrives at the consistent state esteem well ahead of time when contrasted with FDA. It is likewise proven that TDA is precise and mirrors the circuit conduct directly from the main pattern of its working. The nearby correlation of THD, LOH and carrier frequency harmonics for the reproduced and actualized results uncovers the benefit of the proposed method.

References

[1]. Blanes, JM, Garrigos, A, Carrasco, JA, Weinberg, AH, Maset, E, Sanchis-Kilders, E, Ejea, JB &Ferreres, A 2011, 'Two-stage MPPT power regulator for satellite electrical propulsion system', IEEE Transactions on Aerospace and Electronics Systems, vol. 47, no. 3, pp. 1617-1630.

Annals of R.S.C.B., ISSN:1583-6258, Vol. 25, Issue 4, 2021, Pages. 3460 - 3473
Received 05 March 2021; Accepted 01 April 2021.

[2]. Boopathi, R, Muthukumar, P, Melba Mary, P &Jeevananthan, S 2012, ‘Investigation on harmonic spreading effect of switching patterns in VSI fed AC drives’, Proceedings of IEEE International Conference on Advances in Engineering, Science and Management, Nagapattinam, India, vol. 3, pp. 651-656.

[3]. Borisov, K Calvert, TE, Calvert, TE, Kleppe, JA, Martin, E &Trzynadlowski, AM 2006, ’Experimental investigation of a naval propulsion drive model with the PWM-based attenuation of the acoustic and electromagnetic noise’, IEEE Transactions on Industrial Electronics, vol. 53, no. 2, pp. 450-457.

[4]. Bor-Ren Lin &Hsin-Hung Lu 1999, ‘A new control scheme for singlephase PWM multilevel rectifier with power-factor correction’, IEEE Transactions on Industrial Electronics, vol. 46, no. 4, pp. 820-829.

[5]. Brad Lehman & Bass, RM 1996, ‘Switching frequency dependent averaged models for PWM DC-DC converters’, IEEE Transactions on Power Electronics, vol. 11, no. 1, pp. 89-98.

[6]. Busse, DF, Erdman, JM, Kerkman, RJ & Schlegel, DW 1997,‘Bearing current and their relationship to PWM drives’, IEEE Transactions on Industrial Electronics, vol. 12, no. 2, pp. 243–252.

[7]. Cristina Guzman, Alben Cardenas &KodjoAgbossou 2012, ‘Control of voltage source inverter using FPGA implementation of ADALINEFLL’, Proceedings of 38th IEEE Annual Conference on Industrial Electronics, pp. 3037-3042.

[8]. T. Narmadha, J. Gowrishankar, M. Ramkumar, and K. Vengatesan,"Cloud Data Center Based Dynamic Optimizing Replica Migration",J. Comput. Theor. Nanosci. 16, 576–579 (2019)

[9]. Dahidah, MSA &Agelidis, VG 2008, ‘Selective harmonic elimination PWM control for cascaded multilevel voltage source converters: A generalized formula’, IEEE Transactions on Power Electronics, vol. 23, no. 4, pp. 1620-1630.

[10]. Determan, J & Foster, JA 1999, ‘Using chaos in genetic algorithm’, Proceedings of the 1999 Congress on Evolutionary Computation, Washington, DC, vol. 3, pp. 2094-2101.

[11]. Engel, SP, Stieneker, M, Soltau, N, Rabiee, S, Stagge, H & De Doncker, RW 2015, ‘Comparison of the modular multilevel DC converter and the dual-active bridge converter for power conversion in HVDC and MVDC grids’, IEEE Transactions on Power Electronics, vol. 3, no. 1, pp. 124-137.

Annals of R.S.C.B., ISSN:1583-6258, Vol. 25, Issue 4, 2021, Pages. 3460 - 3473
Received 05 March 2021; Accepted 01 April 2021.

[12]. Franc Mihalic&Dejan Kos 2006, ‘Reduced conductive EMI in switched mode DC-DC power converters without EMI filters: PWM versus randomized PWM’, IEEE Transactions on Power Electronics, vol. 21, no. 6, pp. 1783-1794.

[13]. Guo, HY, Li, ZJ, Bo Zhang, Ping Luo& Li, ZH 2008, ‘The effect of duty cycle on suppressing EMI level in random carrier frequency modulation of PWM’, International conference on Apperceiving, Computing and Intelligence Analysis (ICACIA 2008), Chengdu, pp. 164-167.

[14]. Habetler, TG & Divan, DM 1991, ‘Acoustic noise reduction in sinusoidal PWM drives using a randomly modulated carrier’, IEEE Transactions on Power Electronics, vol. 6, pp. 356-363.

[15]. Hamish D Laird, Simon D Round & Richard M Duke 2000, ‘A frequency-domain analytical model of an uncontrolled single-phase voltage-source rectifier’, IEEE Transactions on Industrial Electronics, vol. 47, no. 3, pp. 525-532.